AIP | Journal of Applied Physics

Effects of point defects and dislocations on spectral phonon transport properties of wurtzite GaN

Jinlong Ma, XinJiang Wang, Baoling Huang, and Xiaobing Luo

Citation: J. Appl. Phys. **114**, 074311 (2013); doi: 10.1063/1.4817083
View online: http://dx.doi.org/10.1063/1.4817083
View Table of Contents: http://jap.aip.org/resource/1/JAPIAU/v114/i7
Published by the AIP Publishing LLC.

Additional information on J. Appl. Phys.

Journal Homepage: http://jap.aip.org/
Journal Information: http://jap.aip.org/about/about_the_journal
Top downloads: http://jap.aip.org/features/most_downloaded
Information for Authors: http://jap.aip.org/authors

ADVERTISEMENT

AIPAdvances
Now Indexed in Thomson Reuters Databases
Explore AIP's open access journal:
- Rapid publication
- Article-level metrics
- Post-publication rating and commenting

JOURNAL OF APPLIED PHYSICS 114, 074311 (2013)

Effects of point defects and dislocations on spectral phonon transport properties of wurtzite GaN

Jinlong Ma,[1,2] XinJiang Wang,[2] Baoling Huang,[2,a)] and Xiaobing Luo[1,a)]
[1]*School of Energy and Power Engineering, Huazhong University of Science and Technology, Wuhan 430074, China*
[2]*Department of Mechanical Engineering, Hong Kong University of Science and Technology, Hong Kong, China*

(Received 28 May 2013; accepted 15 July 2013; published online 21 August 2013)

The spectral phonon transport properties of bulk wurtzite GaN are investigated with the Monte Carlo method on the basis of the first principle calculations. Contributions of different phonon modes to the thermal conductivity with respect to the phonon frequency, mean free path, and wavelength are studied and the effects of point defects and dislocations are discussed. It is found that the effects of the dislocations are negligible when the dislocation concentration is below $1 \times 10^{10}\,\mathrm{cm}^{-2}$. The mode analysis shows that the transverse acoustic phonons contribute to the major part of the thermal conductivity from 100 K to 500 K. The point defects and dislocations reduce the thermal conductivity mainly by restraining the transverse modes with little influence on the longitudinal mode. Above 20% thermal conductivity are contributed by phonons with a mean free path larger than 7 μm in pure crystals at near room temperature. For natural crystals with point defects this length will become ever larger, indicating that the size effects should be taken into consideration when the sample characteristic dimension is less than 10 μm. More than 90% thermal conductivity is contributed by phonons with wavelength less than 10 nm for GaN crystals with and without defects, implying that the quantum confinement effect is negligible when the sample characteristic size is larger than 10 nm. © *2013 AIP Publishing LLC*.
[http://dx.doi.org/10.1063/1.4817083]

I. INTRODUCTION

In recent years, GaN has been widely used in electronic and optoelectronic devices, such as light emitting diodes (LED) and high mobility transistors, for its desirable direct band gap and excellent compatibility with silicon structures.[1–5] As the performance and reliability of these devices are very sensitive to temperature, the efficiency of heat removal becomes critical. Therefore, phonon transport properties of GaN have attracted increasing research interest. The thermal conductivities of different GaN samples have been measured over temperature ranges of 10 K–300 K (Refs. 6 and 7) and 4.2 K–300 K.[8,9] These measured values are widely used as fitting object in model analysis of thermal conductivity. Morelli *et al.*[6] used a modified Callaway model to predict the effects of isotopes. The reduction of thermal conductivity of GaN by these isotopes at room temperature was predicted to be about 5%. Slach *et al.*[7] also studied the effects of these isotopes; however, they showed that the thermal conductivity of GaN increased about 11% by eliminating the isotope scattering. Zou *et al.*[10] reported the effects of point impurities and dislocations with the modified Callaway model. Their calculation showed that an increase in doping density from 10^{17} to $10^{18}\,\mathrm{cm}^{-3}$ leaded to a reduction in the thermal conductivity from 177 $\mathrm{Wm}^{-1}\mathrm{K}^{-1}$ to 86 $\mathrm{Wm}^{-1}\mathrm{K}^{-1}$ and the effects of dislocations were significant only as the concentration exceeded $10^{10}\,\mathrm{cm}^{-2}$. Kamatagi *et al.*[11] used the Holland model and a modified Callaway model to analyze the thermal conductivity of different GaN samples. They also studied the low-temperature (from 2 K to 100 K) thermal conductivity of free-standing GaN thin films using a modified Callaway model.[12] Yu *et al.*[13] found that the influence of the point defects and the dislocations was negligible when the concentration of point defects and that of dislocations were below $3 \times 10^{17}\,\mathrm{cm}^{-3}$ and $10^{11}\,\mathrm{cm}^{-2}$, respectively. Zhou *et al.*[14] used a more accurate molecular dynamics method to predict the thermal conductivity of GaN. Alshaikhi *et al.*[15] studied the thermal conductivity of GaN grown with various techniques and found the phonon-impurity scattering played a significant role in determining the thermal conductivity over a very large temperature range. Lindsay *et al.*[16] used the first principle calculation to investigate the phonon transport in GaN and predicted about 65% increase in thermal conductivity with isotope enrichment at room temperature, which is much larger than previous works. Also, the reported thermal conductivity of pure crystals is much higher, meaning that the previous works overestimated the effect of three-phonon scattering.

The studies of phonon transport of GaN in the literatures mainly focus on the total thermal conductivity. However, the detailed information about spectral phonon transport properties of GaN is rarely reported yet. For a better understanding of the phonon transport in GaN, it is quite desirable to figure out how the point defeats and dislocations affect the thermal transport. Meanwhile, the parameters used in the previous theoretical studies are often obtained by directly fitting with the

[a)]Authors to whom correspondence should be addressed. Electronic addresses: Luoxb@hust.edu.cn and mebhuang@ust.hk

 © 2013 AIP Publishing LLC

experimental results, which, however, may be significantly influenced by various defects in the samples and could potentially lead to uncertainties in the modeling. Moreover, although the methods used in previous studies can be used to obtain the thermal conductivity of bulk materials, it is difficult or inefficient to use those methods in multi-scale problems with complex geometries or complicated boundary conditions, especially for multilayer structures or thin films in which both the ballistic and the diffusive transport properties may be important. Considering the advantages of the Monte Carlo method in spatial processing and multi-scale modeling, it is appealing to study the properties with the Monte Carlo method. The Monte Carlo method has been successfully used in the study of phonon transport in bulk material[17] and nanostructures such as thin films,[18–20] nanowires,[21–23] porous structures,[24,25] and nanoparticle composites.[26] The effectiveness and validity of the Monte Carlo method in the multi-scale study of thermal transport have been well confirmed. The work presented here introduces the Monte Carlo method into the simulation for bulk GaN with the use of first principle calculation results. The implementation of Monte Carlo method can be considered as the first step to model the thermal transport in microscale GaN-based devices such as LED chips. In this work, the spectral phonon transport properties of GaN, especially the relative contributions of phonons of different modes, frequencies, mean free paths (MFP) and wavelengths, are studied. The influences of point defects and dislocations on the spectral phonon transport in GaN are also discussed.

II. MONTE CARLO METHODS

A. Theory

The phonon Boltzmann transport equation (BTE) is often used to describe the phonon transport in solids. By adopting the relaxation time approximation, phonon BTE can be simplified as

$$\frac{\partial f}{\partial t} + V_g(\omega, p)\nabla f = -\frac{f - f^{eq}}{\tau(\omega, p, T)}, \tag{1}$$

where V_g is the group velocity, τ is the relaxation time, f is the phonon distribution function, f^{eq} is the equilibrium phonon distribution function, i.e.,

$$f^{eq}(\omega, p, T) = \frac{1}{\exp(\hbar\omega/k_B T) - 1}, \tag{2}$$

where in $\hbar$ is the Planck constant and k_B is the Boltzmann constant. The Monte Carlo method is a statistical method that can be used to solve the BTE by tracking the movement and scattering of the phonons. The phonon transport properties can be obtained by averaging the random movements and scatterings of an enough number of phonons. A brief introduction of the Monte Carlo simulation in phonon transport is discussed below and more details can be referred to previous works.[19,20,24,25]

As the real number of phonons is immense, in the Monte Carlo simulation, each computational particle presents a set of phonons with similar properties. Thus, the effective energy carried by each particle should be chosen first, given as

$$\varepsilon_{eff}^{d} = \frac{V\int_0^{\omega_{\max}} \sum_p \hbar\omega D(\omega, p)|f^{eq}(\omega, p, T) - f^{eq}(\omega, p, T_{ref})|d\omega}{N_{in}}, \tag{3}$$

where ε_{eff}^{d} is the effective energy of each particle, T_{ref} is a selected reference temperature, T is the temperature and N_{in} is the number of particles wanted to be used in the volume of V.

For bulk crystals, the periodic boundary conditions are used. The periodic boundary condition is realized through two steps. First, the particles leaving the system on one side are reinserted on the other side. Second, for isothermal boundary, new particles generated in each time step, Δt. The number of new particles is determined by

$$N_b = \frac{A\Delta t}{4\varepsilon_{eff}^{d}} \int_0^{\omega_{\max}} \sum_p \hbar\omega D(\omega, p) V_g(\omega, p)|f^{eq}(\omega, p, T_{high}) - f^{eq}(\omega, p, T_{low})|d\omega, \tag{4}$$

where T_{high} is the temperature of the hot boundary and T_{low} is the temperature of the cold boundary.

After the number of particles is known, their properties such as frequency, velocity, polarization, locations and direction need to be decided. A cumulative energy density function of phonons over frequency spectrum is constructed as

$$F_i = \sum_{j=1}^{i} E_j \Big/ \sum_{j=1}^{N} E_j, \tag{5}$$

where

$$E_j = \sum_p \hbar\omega_j D(\omega_j, p)[f^{eq}(\omega_j, p, T) - f^{eq}(\omega_j, p, T_{ref})]\Delta\omega. \tag{6}$$

Here N is the number of frequency spectrum divided, and $\Delta\omega = \omega_{\max}^{LA}/N$. Then a random number R_ω is generated to decide the frequency of the particle by making it satisfy the relation $F_{i-1} < R_\omega \le F_i$. After the frequency of computational particle is known, the polarization probabilities can be determined by computing the ratio of the phonon energy of each branch to the total phonon energy in the ω_i interval

$$P_{p_j,i} = \sum_{j=1}^{j} E_i(\omega_i, p_j) \Big/ \sum_{j=1}^{3} E_i(\omega_i, p_j). \tag{7}$$

Then a random number, R_p, is used to select the polarization like what is done in the frequency determination. Once the frequency and polarization are decided, the group velocity is determined by the phonon dispersion. The velocity directions of a particle are selected randomly (isotropy assumption).

The important part of the Monte Carlo method is to track the movement of the particles step by step. At the end of each time step, scatterings are considered. As the scattering rates are related to temperature and the temperature distribution

varies with the movement of particles, the temperature should be updated at the end of each time step according to the formula

$$\frac{\Delta E_j}{V_j} = \int_0^{\omega_{\max}} \sum_p \hbar\omega D(\omega.p)[f^{eq}(\omega,p,T_j) - f^{eq}(\omega,p,T_{ref})]d\omega. \quad (8)$$

After the temperature is known, the relaxation time, $\tau(\omega_i,p,T_j)$, can be calculated. A scattering probability $P_{scat} = 1 - \exp(-\Delta t/\tau)$ is constructed to decide whether the particle experience a scattering. If the particle is scattered, its properties are reset; otherwise, its properties are kept the same.

When the system becomes stable, the thermal conductivity can be directly determined by the heat flux through the medium and the temperature difference according to Fourier's law. The heat flux along the temperature gradient is calculated according to

$$q = \frac{1}{V}\sum_i^N e_i \langle \vec{V}_g(i)\cdot\vec{k}\rangle, \quad (9)$$

where e_i is the particle energy, and $\langle \vec{V}_g(i)\cdot\vec{k}\rangle$ represents the velocity along the temperature gradient.

B. Phonon dispersion relation

Phonon state is described by phonon dispersion relation. It is ideal to consider the complete phonon dispersion relation for an accurate simulation. However, considering the complete set of phonon states is too complex and cumbersome in many cases. Since optical phonons generally contribute little to the thermal conductivity, following previous studies,[6,10–13] only the contributions of acoustic phonon modes are considered in this work. The first principle calculation results[16] also show that the thermal conductivity of wurtzite GaN along the in-plane (*a*, *b* axis) direction only differ 3% from that along the out-of-plane (*c* axis) direction. Consequently, the thermal transport properties of wurtzite GaN are almost isotropic.

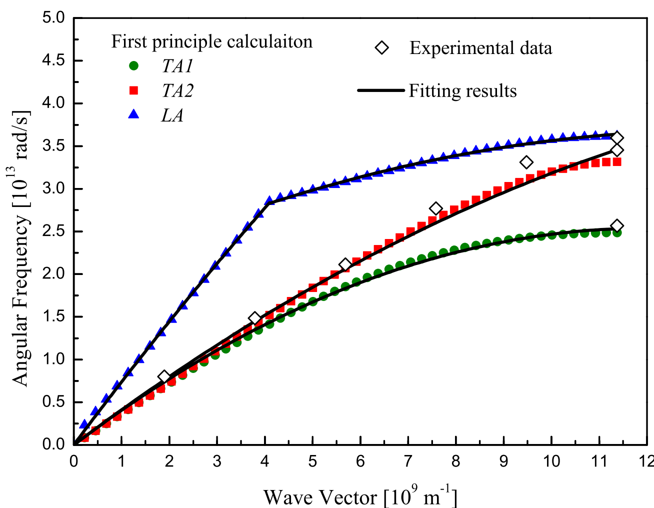

FIG. 1. Phonon dispersion relation of wurtzite GaN in the Γ-M direction.

Therefore, the phonon dispersion in the Γ-M direction can be used to represent all dispersions.[6,11] The phonon dispersion of wurtzite GaN used in this work is shown in Fig. 1. It is obtained from the first principle calculation and is in good agreement with other first principle calculation results[16,27] and the experiment data of inelastic x-ray scattering.[27] There are two non-degenerate transverse acoustic branches (*TA*1 and *TA*2) and one longitudinal acoustic branch (*LA*). A quadratic expression is used to fit the dispersion data. As in GaN, the frequency of some optical phonon modes is relatively low and can suppress the *LA* branch. Thus, the gradient of the longitudinal branch changes significantly in the former half and the latter half, it is divided into two parts during the fitting. The fitting results are show as follows:

$$\begin{aligned}
TA1:\ & \omega = 0 + 4.222\times10^3 k - 1.755\times10^{-7}k^2,\\
TA2:\ & \omega = 0 + 4.205\times10^3 k - 1.023\times10^{-7}k^2,\\
LA:\ & \omega = 0 + 7.512\times10^3 k - 1.432\times10^{-7}k^2,\\
& k <= 0.36k_{\max},\\
& \omega = 1.930\times10^{13} + 2.583\times10^3 k - 0.949\times10^{-7}k^2,
\end{aligned} \quad (10)$$

where k is the wave vector and ω is the angular frequency. The maximum wave vector $k_{\max} = 11.375\times10^9\ \mathrm{m}^{-1}$.

C. Relaxation times

The scattering processes which limit thermal conduction include the scatterings by boundaries, impurities, isotopes, dislocations, and other phonons. In this work, we mainly consider the phonon-phonon scattering, phonon-point defect scattering and phonon-dislocation scattering. While the phonon-phonon scattering is intrinsic, the other scattering mechanisms are sample-dependent.

In the Monte Carlo simulation, the phonon relaxation times limited by various scattering mechanisms need to be known in advance. And they are always obtained by adjusting the relaxation time parameters until the calculation results are in agreement with experimental data. However, as the experimental samples are not free of defects, the relaxation time of the intrinsic scattering, which is mainly three-phonon scattering including the normal processes (N) and the Umklapp processes (U), is difficult to separate from those of other scatterings. This may lead to large uncertainty in the prediction. Fortunately, the thermal conductivity of pure GaN can be obtained from the first principle calculation.[16] Thus, by fitting with the thermal conductivity of pure GaN calculated from the first principle, more accurate three-phonon relaxation time can be obtained separately. Following the previous studies, the three-phonon relaxation times of different phonon modes in N processes and U processes can be formulated as[6,11,12,28]

$$\begin{aligned}
(\tau_{TA}^N)^{-1} &= B_{TA}^N \omega T^4,\\
(\tau_{LA}^N)^{-1} &= B_{LA}^N \omega^2 T^3,\\
(\tau_{TA}^U)^{-1} &= B_{TA}^U \omega^2 T\exp(-\theta_{TA}^D/3T),\\
(\tau_{LA}^U)^{-1} &= B_{LA}^U \omega^2 T\exp(-\theta_{LA}^D/3T),
\end{aligned} \quad (11)$$

where the subscripts TA and LA indicate transverse and longitudinal acoustic modes, respectively, the superscripts N and U represent N processes and U processes, $B_{TA}^{N}, B_{LA}^{N}, B_{TA}^{U}$, and B_{LA}^{U} are adjustment parameters, and θ^{D} is the Debye temperature. This work does not make a distinction between N process and U process. They are treated as isotropic three-phonon scattering,[19,20,22,24,29] i.e., $(\tau_s^{NU})^{-1} = (\tau_s^{N})^{-1} + (\tau_s^{U})^{-1}$.

The point-defect relaxation time is as follows:[6,12]

$$(\tau_s^{I})^{-1} = B_s^{I}\omega^4, \tag{12}$$

where B_s^{I} is the fitting parameters of the corresponding modes.

The three-phonon relaxation times are obtained by fitting with the results of the first principle calculation for pure crystals,[16] which is free of defects. Then the point-defect relaxation time is obtained by fitting the experimental data of natural crystals.[6,7] As the defects of natural crystals are the combination of different element impurities and their isotopes, for simplicity, the point-defect scattering considered in this work reflects the overall effects. The fitted adjustment parameters are listed in Table I. As the dispersion relation and the thermal conductivities used in this work are different, the magnitude of the parameters for scattering rate differ from previous works.[6,11] However, the parameters for U processes which are the main thermal resistance are at the same order. With this set of parameters, the coincidence of the calculated thermal conductivity with the first principle results and experimental data is shown in Fig. 2.

The phonons can also be scattered by the cores of dislocation lines or by the strain fields surrounding the dislocation lines. The relaxation time limited by the cores of dislocation lines is given by[10,12]

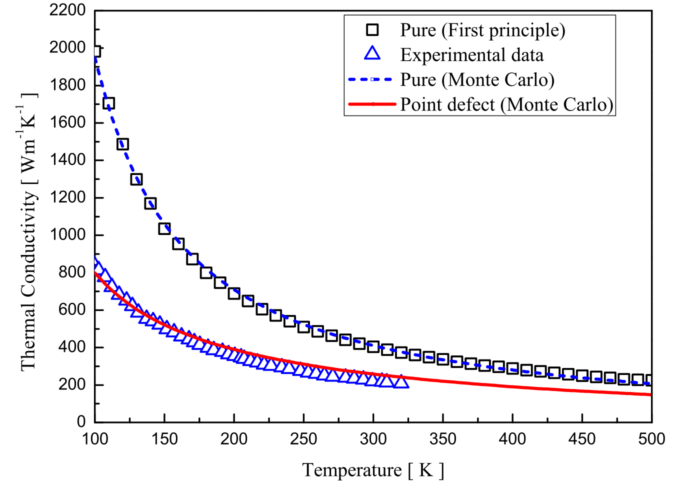

FIG. 2. The thermal conductivity of wurtzite GaN calculated with the Monte Carlo method.

$$(\tau_s^{CD})^{-1} = \eta N_{dis}\frac{{V_0}^{4/3}}{v_s^2}\omega^3, \tag{13}$$

where N_{dis} is the dislocation concentration and η is the mutual orientation of the temperature gradient and dislocation line. For dislocations perpendicular to the temperature gradient $\eta = 1$ while for dislocation parallel to the gradient $\eta = 0$, and for random orientation $\eta = 0.55$.

There are mainly three kinds of dislocations: screw, edge, and mixed dislocations. The relaxation times caused by the strain field associated with them are expressed as[10,12]

$$\begin{aligned}
(\tau_s^{SD})^{-1} &= \frac{2^{3/2}}{3^{7/2}}\eta N_{dis}^{SD} b_S^2\gamma_s^2\omega, \\
(\tau_s^{ED})^{-1} &= \frac{2^{3/2}}{3^{7/2}}\eta N_{dis}^{ED} b_E^2\gamma_s^2\omega\left\{\frac{1}{2}+\frac{1}{24}\left(\frac{1-2\upsilon}{1-\upsilon}\right)^2\left[1+\sqrt{2}\left(\frac{v_L}{v_T}\right)^2\right]^2\right\}, \\
(\tau_s^{MD})^{-1} &= \frac{2^{3/2}}{3^{7/2}}\eta N_{dis}^{MD}\gamma_s^2\omega\left(b_S^2+b_E^2\gamma^2\omega\left\{\frac{1}{2}+\frac{1}{24}\left(\frac{1-2\upsilon}{1-\upsilon}\right)^2\left[1+\sqrt{2}\left(\frac{v_L}{v_T}\right)^2\right]^2\right\}\right),
\end{aligned} \tag{14}$$

where $N_{dis}^{SD}, N_{dis}^{ED}$ and N_{dis}^{MD} are the concentrations of the screw, edge and mixed dislocations, respectively, and the total dislocation concentration is $N_{dis} = N_{dis}^{SD} + N_{dis}^{ED} + N_{dis}^{MD}$. For simplification, the densities of the three types of dislocations are assumed equal.[10] The Grüneisen parameters for the transverse and the longitudinal acoustic modes are 0.45 and 1.1, respectively.[11,12] υ is Poisson's ratio and its value is 0.37 for GaN.[10] $b_S = c$ and $b_E = a\sqrt{2}/3$, wherein a and c are lattice constants.

The expressions about the dislocation scattering above just apply for independent dislocation lines.[30] However, when the dislocation concentration is high, the changes in the individual linkage of the immediate vicinity of each dislocation line should be considered owing to the short spacing. The corresponding relaxation time is expressed as[11,12]

$$\left(\tau_s^{DO}\right)^{-1} = \frac{c^2a^3N_d^2\eta\gamma_s^2\omega^2}{v_s}. \tag{15}$$

III. RESULTS

A. Effect of dislocation concentration

As mentioned above, the dislocation relaxation times are related to the dislocation concentration. Thus, the influence

TABLE I. Fitted parameters of the relaxation times for the three-phonon scattering and the point-defect scattering.

$B^N_{TA}[\mathrm{K}^{-4}]$	$B^N_{LA}[\mathrm{sK}^{-3}]$	$B^U_{TA}[\mathrm{sK}^{-1}]$	$B^U_{LA}[\mathrm{sK}^{-1}]$	$B^I_{TA}[\mathrm{s}^3]$	$B^I_{LA}[\mathrm{s}^3]$
3.26×10^{-16}	4.12×10^{-27}	3.85×10^{-20}	5.31×10^{-20}	3.73×10^{-44}	5.21×10^{-45}

of the dislocation concentration is studied first. Figure 3 shows the dependence of the thermal conductivity on the dislocation concentration at 300 K. The solid line represents the thermal conductivity of pure crystals, while the dashed line is for natural crystals. As the concentration increases, the thermal conductivity reduces. There is a critical concentration below which the thermal conductivity is little influenced. The dislocation concentrations corresponding to 5% reduction in the thermal conductivity at 300 K are $5 \times 10^{10}\,\mathrm{cm}^{-2}$ and $1 \times 10^{11}\,\mathrm{cm}^{-2}$ for pure and natural crystals, respectively. For natural crystals which include point defects, the critical concentration is larger. When the concentration exceeds the critical value, the thermal conductivity of natural crystals is less sensitive to dislocation concentration than that of pure crystals, which is due to the decrement of the relative contribution of dislocation scattering to thermal resistance. In the following discussion, in order to clarify the effects of dislocations on the spectral phonon transport properties, the dislocation concentration is deliberately set as $5 \times 10^{11}\,\mathrm{cm}^{-2}$, which causes obvious thermal conductivity reduction.

B. Contributions of different modes

Figure 4 shows the contributions of different acoustic phonon modes to the thermal conductivity from 100 K to 500 K. In this temperature range, the two *TA* modes dominate the thermal transport in pure crystals and contribute about 80% of the thermal conductivity. The contribution from the *LA* mode is about 20% near the room temperature but its relative contribution increases a little with the increase in temperature, as the *TA* modes are more sensitive to the three-phonon scattering. However, for GaN crystals with point defects or dislocations, the results may be quite different. Figure 4 also shows the contributions from the different modes to the thermal conductivity for GaN crystals when the effects of point defects (Fig. 4(a)) and dislocations (Fig. 4(b)) are considered. Both point defects and dislocations can reduce the thermal conductivity mainly by suppressing the contributions from the *TA* modes while almost no effect on the *LA* mode is observed above the room temperature. At low temperatures, it seems that the dislocations have a significant influence on all the modes while point defects mainly affect the *TA* modes. Consequently, the relative contribution to the total thermal conductivity by the *LA* mode becomes larger. The influence of point defects and dislocations is relatively stronger at lower temperatures, because the three-phonon scattering becomes weaker as the temperature decreases. It can be found that the dislocations under the selected concentration cause almost the same reduction on thermal conductivity as the point defects (154 and 157 $\mathrm{Wm}^{-1}\mathrm{K}^{-1}$, respectively) at 300 K. This means the effect of point defects and dislocations at 300 K are comparable in the following discussion.

C. Frequency dependence

The contributions of phonons with different frequencies to the thermal conductivity at 300 K are shown in Fig. 5. The solid line indicates the spectral contributions for pure crystals. There are three obvious turning points in the contribution spectrum, corresponding to the cutoff frequency of the *TA*1 mode, the turning point frequency of the *LA* mode and the cutoff frequency of the *TA*2 mode, respectively. About 90% thermal conductivity is contributed by phonons with frequency less than 4.5 THz, close to the turning point of *LA*. In the frequency range from 0.5 THz to 4 THz, the contributions from phonons with different frequencies are almost equal. The introduction of point defects and dislocations may significantly affect the contributions of phonons with

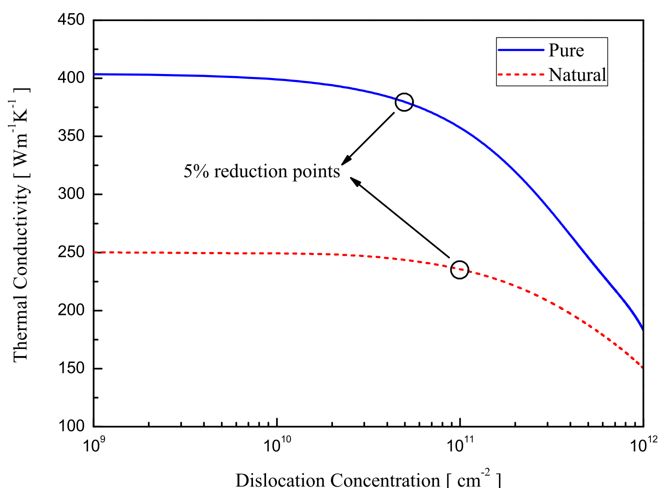

FIG. 3. Variation of the thermal conductivity with respect to dislocation concentration.

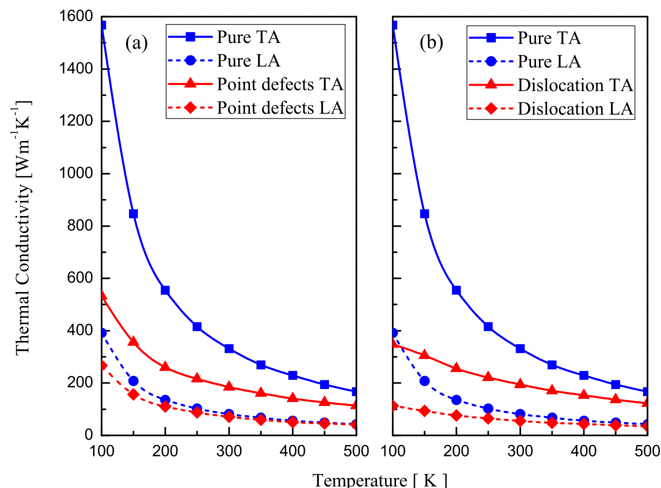

FIG. 4. Effects of point defects (a) and dislocations (b) on the thermal conductivity contributions of different modes in wurtzite GaN.

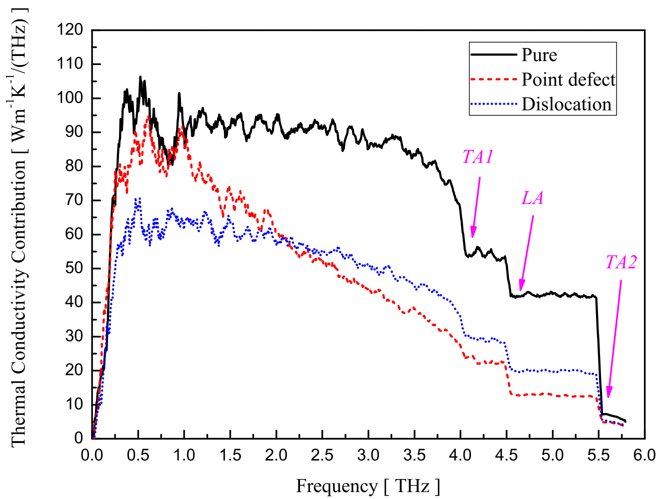

FIG. 5. Contribution to the phonon thermal conductivity with respect to phonon frequency for pure GaN crystals and GaN crystals with point defects and dislocations at 300 K.

different frequencies. As shown in Fig. 5, it is clear that the point defects remarkably reduce the contributions of high-frequency phonons with little effects on low-frequency phonons (below 1 THz). In contrast, the dislocations affect acoustic phonons over the entire spectrum with slightly more influence on high-frequency phonons. This is due to the fact that the point-defect scattering is proportional to ω^4, while the dislocation scattering is related to ω, ω^2 and ω^3. In natural crystals, the low-frequency phonons contribute more than that in pure crystals. About 90% thermal conductivity is attributed by the phonons with a frequency below 4.0 THz.

Figure 6 shows the MFP distribution with respect to phonon frequency for pure GaN crystals and GaN crystals with point defects and dislocations. As for pure crystals, even though there are three turning points, overall the mean free path decreases with the increase in frequency. It can be seen that when the point defects are considered, MFPs of high-frequency phonons decrease further while those of low-frequency phonons (below 1 THz) almost remain the same. This further clarify the point defects have little effect on low-frequency phonons. In contrast, the introduction of dislocations decreases the MFP of phonons over the entire spectrum.

D. Phonon mean free path dependence

Since GaN used in many electronic and optoelectronic devices are in the form of thin films, to understand the size effects on the thermal transport, the contributions to phonon thermal conductivity with respect to MFP at different temperatures are calculated and shown in Fig. 7. Figure 7(a) shows the results for pure crystals at 100 K, 300 K, and 500 K and apparently the corresponding peak contribution comes from phonons with a MFP of about 1000 nm, 200 nm, and 100 nm, respectively. Note that the thermal conductivity corresponds to the area under the contribution curve. Although at lower temperatures the peak contribution magnitude is lower, phonons with a long MFP contribute much more to the thermal transport, leading to a higher thermal conductivity. As temperature increases, the contribution distribution shifts to the left and the contribution peak magnitude increases, indicating that the relative contributions from phonons with a short MFP increase. This is because the stronger phonon-phonon scattering shortens the phonon MFP and results in more short-MFP phonons contributing to the thermal transport. However, even at high temperatures, phonons of a long MFP still contribute significantly to the total thermal conductivity. About 20% thermal conductivity is contributed by phonons with a MFP longer than 42 μm, 7 μm, and 2.6 μm at 100 K, 300 K, and 500 K, respectively. This indicates that the classical size effects may play an important role in determining the thermal conductivity of pure GaN thin films when their film thicknesses are below a few microns. As temperature increases, the size effects MFP become weaker. Figures 7(b) and 7(c) show the results for GaN crystals with point defects and those with dislocations, respectively. Compared with the results for pure crystals, the point defects significantly shift the contribution curve to the left side with slight decrease in the peak magnitude. For natural crystals at 300 K, phonons with a MFP larger than 12.5 μm still contribute about 20% to

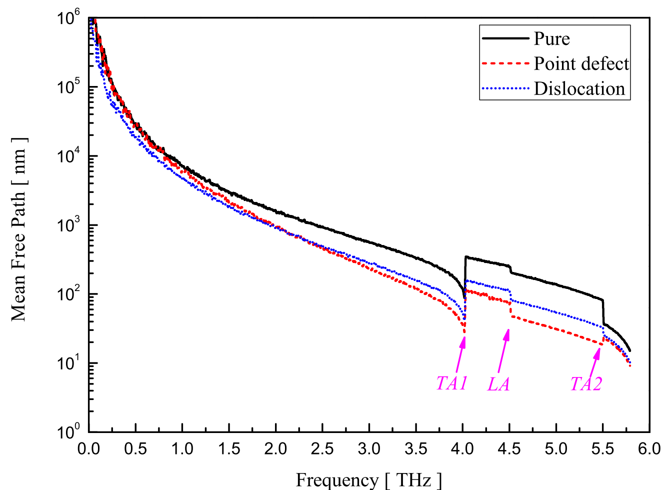

FIG. 6. Phonon mean free path with respect to frequency for pure GaN crystals and GaN crystals with point defects and dislocations at 300 K.

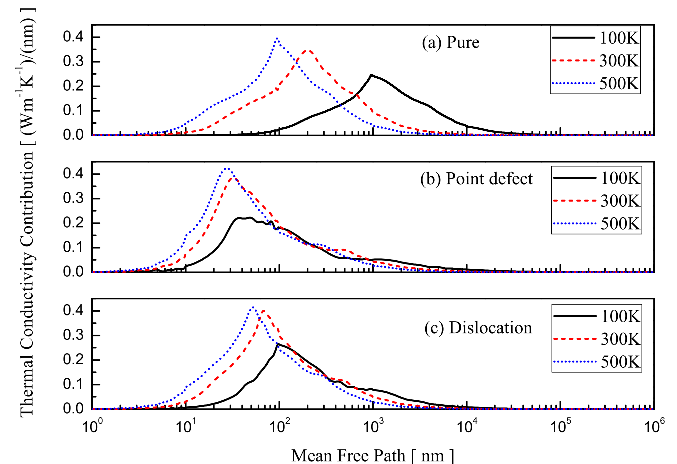

FIG. 7. Contribution to the phonon thermal conductivity with respect to phonon MFP for (a) pure GaN crystals and GaN crystals with (b) point defects and (c) dislocations at different temperatures.

the thermal conductivity. This value is larger than that for the pure crystals. The reason lies in that point defects mainly affect the high-frequency phonons with weaker influence on low-frequency phonons, which generally have a long MFP. This means the relative contributions by phonons with a long MFP increase although the point defects reduce the total thermal conductivity. This indicates that although the point defects can reduce phonon MFP, they also make the total thermal conductivity more sensitive to the sample characteristic length. The classical size effects should be taken into consideration when the characteristic dimension of samples is below 10 μm. In contrast, the dislocations shorten this value to 6 μm at 300 K, indicating the dislocations reduce the thermal conductivity and make the size effects weaker.

In order to have a clearer sight into the influence of those defects on the different modes, the contributions to the thermal conductivity by different modes at 300 K with respect to the phonon MFP are calculated for pure crystals and samples with point defects and dislocations, as shown in Fig. 8. It can be seen that the MFPs of the three modes in all the cases span a wide range from 10 nm to 10 μm. In pure crystals, apparently the *TA* modes contribute to the major part of the thermal conductivity and the contribution peaks at a mean free path of around 200 nm at 300 K. In contrast, the *LA* mode contributes much less and its major contribution is from phonons in the short MFP regime. The contribution of the *LA* mode peaks at a mean free path of around 50 nm. Comparing the contribution distributions with and without point defects, the point defects shift the contribution curve of *TA* modes to the left side while reducing the peak contribution magnitude. The point defects change many *TA* phonons of long MFP into phonons of short MFP; therefore, the contribution by phonons with short MFP increases and the contribution peaks at a mean free path of around 30 nm. Meanwhile, it seems that the scattering by point defects only slightly affects the *LA* mode. As shown in Fig. 8(b), the influence of dislocations also focuses on *TA* modes and the net effect is to shift the *TA* contribution curve to the left side (shorter MFP).

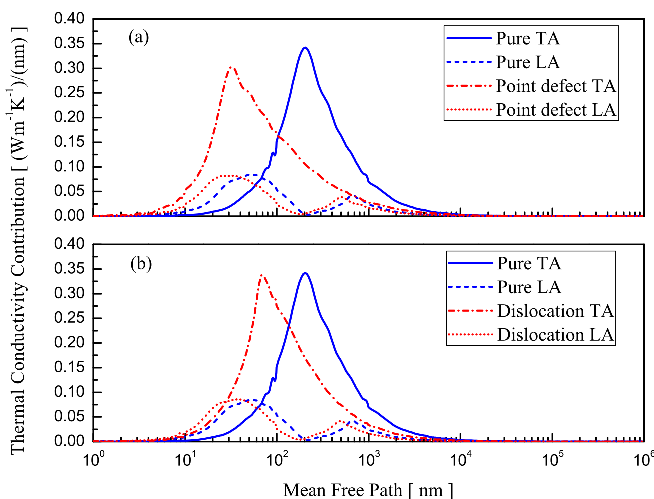

FIG. 8. Contributions of the *TA* and *LA* modes to phonon thermal conductivity with respect to phonon MFP at 300 K for GaN crystals with (a) point defects and (b) dislocations.

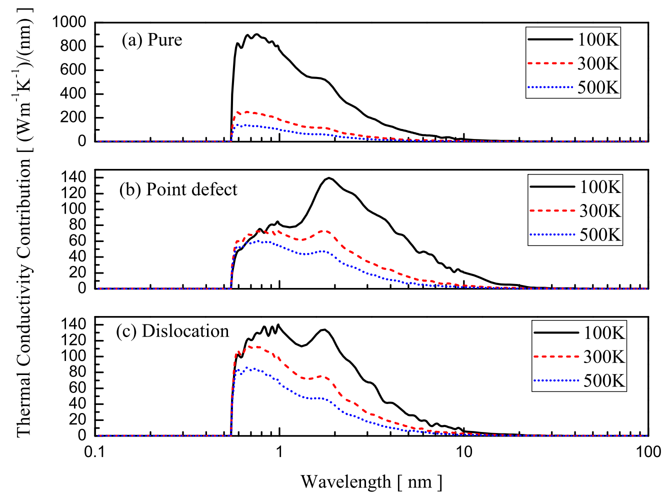

FIG. 9. Contributions to the phonon thermal conductivity with respect to phonon wavelength at different temperatures for (a) pure GaN crystals and GaN crystals with (b) point defects and (c) dislocations.

E. Phonon wavelength dependence

For low-dimensional structures such as thin films, the constrained dimension will limit the available phonon modes, therefore changing the phonon dispersion relations. It is desirable to clarify this quantum confinement effects on the phonon transport for the application of these structures. Figure 9 shows the contributions to the phonon thermal conductivity with respect to phonon wavelength at different temperatures. Apparently, major part of the thermal conductivity is contributed by phonons of a short wavelength. Figure 9(a) shows that, for pure crystals, acoustic phonons with a wavelength below 10 nm contribute more than 90% of the total thermal conductivity from 100 K to 500 K. Even for natural crystals and samples with dislocations, as shown in Figs. 9(b) and 9(c), the corresponding contributions are still more than 90%. It means that for samples of a characteristic dimension above 10 nm, the effects of quantum confinements are negligible and only classical size effects need to be taken into the consideration. The dominant range of wavelength does not vary much with the variation in temperature. Meanwhile, Figs. 9(b) and

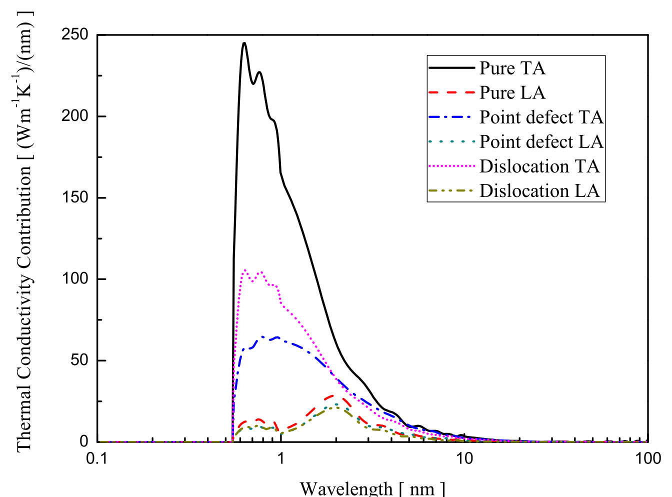

FIG. 10. Contributions of the *TA* and *LA* modes to phonon thermal conductivity with respect to phonon wavelength at 300 K for GaN crystals.

9(c) show that both point defects and dislocations have a noticeable influence on the contribution of short-wavelength phonons especially when the temperature is low, because these phonons are generally of a high frequency. Figure 10 shows the contributions to the thermal conductivity by different modes at 300 K. It is clear that the point defects and the dislocations mainly influence the transverse modes with minor effects on the longitudinal mode. Again, their impacts mainly focus on short-wavelength transverse phonons.

IV. CONCLUSIONS

In this work, the Monte Carlo method has been implemented to investigate the spectral phonon transport properties of wurtzite GaN. Based on the results of the first principle calculations and the experiment data, a set of parameters for scattering relaxation times are obtained. The study on the effects of dislocation concentration shows that the reduction of thermal conductivity is less than 1% by constraining the concentration below $1 \times 10^{10}\,\mathrm{cm}^{-2}$. Through the analysis on the contribution of different modes to the thermal conductivity, it is found that the transverse mode is the main contributor. The point defects and dislocations can reduce the thermal conductivity mainly by affecting the transverse modes with little influence on the longitudinal mode above room temperature. The contributions to the thermal conductivities with respect to phonon frequency, MFP and wavelength have been calculated. While the point defects mainly affect high-frequency phonons, the dislocations have a remarkable influence on phonons over the entire spectrum. About 90% of the thermal conductivity is contributed by phonons with a frequency lower than 4.5 THz and 4.0 THz for pure crystals and natural crystals, respectively. The MFP of phonons that contribute noticeably to the thermal conductivity of GaN ranges from 10 nm to 10 μm near room temperature. Above 20% thermal conductivity is contributed by phonons with a MFP above 12.5 μm for natural crystals and the corresponding MFP value for pure crystals is 7 μm. This indicates the classical size effect should be taken into the consideration as the characteristic dimension is below 10 μm. The major part of the thermal conductivity is contributed by the phonons of a wavelength below 10 nm even when the point defects and the dislocations are introduced. Therefore, the quantum confinement effects on phonon dispersions can be neglected when the sample characteristic dimensions are larger than 10 nm. The point defects and dislocations mainly suppress the transverse acoustic phonons with a short wavelength.

ACKNOWLEDGMENTS

The authors would like to acknowledge the financial support in part from 973 Project of The Ministry of Science and Technology of China (2011CB013105), in part by National 863 project of The Ministry of Science and Technology of China (2011AA03A109).

[1]S. N. Mohammad, A. A. Salvador, and H. Morkoc, Proc. IEEE **83**, 1306 (1995).
[2]K. Chung, C.-H. Lee, and G.-C. Yi, Science **330**, 655 (2010).
[3]S. J. Pearton, J. C. Zolper, R. J. Shul, and F. Ren, J. Appl. Phys. **86**, 1 (1999).
[4]S. T. Sheppard, K. Doverspike, W. L. Pribble, S. T. Allen, J. W. Palmour, L. T. Kehias, and T. J. Jenkins, IEEE Electron Device Lett. **20**, 161 (1999).
[5]P. B. Klein, J. J. A. Freitas, S. C. Binari, and A. E. Wickenden, Appl. Phys. Lett. **75**, 4016 (1999).
[6]D. T. Morelli, J. P. Heremans, and G. A. Slack, Phys. Rev. B **66**, 195304 (2002).
[7]G. A. Slack, L. J. Schowalter, D. Morelli, and J. A. Freitas, Jr., J. Cryst. Growth **246**, 287 (2002).
[8]A. Jeżowski, B. A. Danilchenko, M. Boćkowski, I. Grzegory, S. Krukowski, T. Suski, and T. Paszkiewicz, Solid State Commun. **128**, 69 (2003).
[9]A. Jeżowski, P. Stachowiak, T. Plackowski, T. Suski, S. Krukowski, M. Boćkowski, I. Grzegory, B. Danilchenko, and T. Paszkiewicz, Phys. Status Solidi B **240**, 447 (2003).
[10]J. Zou, D. Kotchetkov, A. A. Balandin, D. I. Florescu, and F. H. Pollak, J. Appl. Phys. **92**, 2534 (2002).
[11]M. D. Kamatagi, N. S. Sankeshwar, and B. G. Mulimani, Diamond Relat. Mater. **16**, 98 (2007).
[12]M. D. Kamatagi, R. G. Vaidya, N. S. Sankeshwar, and B. G. Mulimani, Int. J. Heat Mass Transfer **52**, 2885 (2009).
[13]X.-G. Yu and X.-G. Liang, Diamond Relat. Mater. **16**, 1711 (2007).
[14]X. W. Zhou, S. Aubry, R. E. Jones, A. Greenstein, and P. K. Schelling, Phys. Rev. B **79**, 115201 (2009).
[15]A. AlShaikhi, S. Barman, and G. P. Srivastava, Phys. Rev. B **81**, 195320 (2010).
[16]L. Lindsay, D. A. Broido, and T. L. Reinecke, Phys. Rev. Lett. **109**, 095901 (2012).
[17]D. Lacroix, K. Joulain, and D. Lemonnier, Phys. Rev. B **72**, 064305 (2005).
[18]A. Mittal and S. Mazumder, J. Heat Transfer **132**, 052402 (2010).
[19]S. Mazumder and A. Majumdar, J. Heat Transfer **123**, 749 (2001).
[20]B. T. Wong, M. Francoeur, and M. Pinar Mengüç, Int. J. Heat Mass. Transfer **54**, 1825 (2011).
[21]Y. F. Chen, D. Li, J. R. Lukes, and A. Majumdar, J. Heat Transfer **127**, 1129 (2005).
[22]E. B. Ramayya, L. N. Maurer, A. H. Davoody, and I. Knezevic, Phys. Rev. B **86**, 115328 (2012).
[23]D. Lacroix, K. Joulain, D. Terris, and D. Lemonnier, Appl. Phys. Lett. **89**, 103104 (2006).
[24]Q. Hao, G. Chen, and M.-S. Jeng, J. Appl. Phys. **106**, 114321 (2009).
[25]J. -P. M. Péraud and N. G. Hadjiconstantinou, Phys. Rev. B **84**, 205331 (2011).
[26]M.-S. Jeng, R.-G. Yang, D. Song, and G. Chen, J. Heat Transfer **130**, 042410 (2008).
[27]T. Ruf, J. Serrano, M. Cardona, P. Pavone, M. Pabst, M. Krisch, M. D'Astuto, T. Suski, I. Grzegory, and M. Leszczynski, Phys. Rev. Lett. **86**, 906 (2001).
[28]M. Asen-Palmer, K. Bartkowski, E. Gmelin, M. Cardona, A. P. Zhernov, A. V. Inyushkin, A. Taldenkov, V. I. Ozhogin, K. M. Itoh, and E. E. Haller, Phys. Rev. B **56**, 9431 (1997).
[29]J. Randrianalisoa and D. Baillis, J. Heat Transfer **130**, 072404 (2008).
[30]P. Klemens, Proc. Phys. Soc., London, Sect. A **68**, 1113 (1955).